Evaluation of the ultrasonic transducer electrical matching performance

L.Svilainis, V. Dumbrava

Signal processing department, Kaunas University o f Technology,
Studentu str. 50, LT-51368 Kaunas, Lithuania, tel. +370 37 300532, E-mail.:svilnis@ktu.lt

Abstract

Performance of electrical matching of an ultrasonic transducer to the excitation generator is analyzed. The analysis is based on a transducer measured impedance. Real power supplied to the ultrasonic transducer is one of evaluation criteria. The obtainable bandwidth as well as it's product with a real power supplied are assigned as the alternative performance evaluation criteria. Effective bandwidth is adopted from radiolocation as one of criteria. Most popular matching circuits are analyzed using the mentioned criteria. Algorithms for matching network selection are presented.

Keywords: Ultrasonic transducer impedance, impedance matching, power factor

Introduction

The transducer electrical impedance affects an ultrasonic transducer noise performance, driving response, bandwidth and sensitivity [1-3]. These parameters can be modified by applying the electrical circuit in between the ultrasonic transducer and the excitation generator. Convenient approach to predict the result of such circuit introduction is to approximate the ultrasonic transducer by some electrical model [4]. In many instances optimal tuning circuit search is based on the Butterworth-Van-Dyke (BVD) model [5]. According to [6] BVD and Redwood models are derived by simplifying the Mason equivalent circuit and can be made by piezoelectric impedance modeling based on experimental results and electromechanical analogies. We consider BVD as the best lumped parameter equivalent circuit suitable for our purpose since they are fitting typical piezoelectric transducer impedance and are able to represent the transduction. The capacitance of the piezoelectric material is represented by C_0. The mechanical system is described by a series resonant circuit L_m, C_m, R_m. Changes in the mechanical boundary conditions are modeled by alteration of R_m, and C_m, while changes of inductance L_m describing the mass of the mechanical system, generally can be neglected. The R_m is an emission resistance [7]. The R_m, can be split:

$$R_m = R_{lm} + R_{xm}, \quad (1)$$

where R_{lm} is the part representing the losses in piezo-ceramic material and R_{xm}- acoustic transmission into the medium. Assuming that losses in transducer are relatively small, the power supplied to R_m can be considered as the transducer acoustic emission.

The impedance Z_T of an ultrasonic transducer then can be expressed as [8]:

$$Z_T = \frac{\left(\omega^2 C_m L_m - 1 j\omega L_m\right) - j\left(\omega C_m R_m\right)}{\left(\omega^2 C_0 C_m R_m\right) + j\left[\omega^3 C_0 C_m L_m - \omega\left(C_0 + C_m\right)\right]}. \quad (2)$$

In such case the transducer will exhibit serial and parallel resonances:

$$\omega_s = \frac{1}{\sqrt{L_m C_m}}, \omega_p = \sqrt{\frac{C_m + C_0}{L_m C_m C_0}}, \frac{\omega_p}{\omega_s} = \sqrt{1 + \frac{C_m}{C_0}}. \quad (3)$$

The series resonance frequency of such mechanical system is the optimal point of operation, because the oscillation magnitude is reaching its maximum value. For increase of emission efficiency matching circuits are used.

The aim of this work is to analyze the matching techniques performance based on the measured transducer impedance instead of BVD model.

Matching circuits

The power delivered to a load is maximized when the load impedance is equal to the generator intrinsic resistance R_g. At the serial resonance the complex impedance of L_m, C_m series connection is zero and the equivalent transducer circuit is simplified to parallel connection of R_m and C_0 (Fig.1). It is evident that the power supplied to the transducer is tampered by the capacitance of the piezoelectric transducer C_0 This capacitance is loading the excitation generator output and is reducing the generator efficiency.

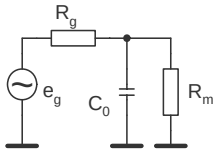

Fig. 1. **Equivalent circuit at mechanical resonance**

Ideally an element with the value $-C_0$ should be placed in parallel to the transducer. Two simple methods exist to compensate for this capacitance: parallel or serial connection of inductance [9]. It should be noted that compensation is available only at a single frequency. But for many applications such compensation is sufficient.

Parallel compensating inductor (Fig.2). If matching performed at the mechanical resonance frequency, then L_m, C_m series connection is zero and only R_m and C_0 are used for calculation.

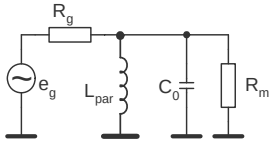

Fig. 2**. Equivalent circuit with parallel compensating inductance**

The parallel L_{par} inductance value then is calculated as:

$$L_{par} = \frac{1}{(\omega_s)^2 C_0}. \quad (4)$$

It should be noted that inductor's quality will affect the compensation results. Every real inductor can be treated as a serial connection of an ideal inductance and a losses resistance (refer Fig.3).

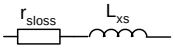

Fig. 3. **Equivalent circuit of lossy inductor**

The series connection of L_{xs} and r_{sloss} can be converted to the parallel inductance L_{xp} and the loss resistance r_{ploss} [10]:

$$Q_L = \frac{2\pi f L_{xs}}{r_{sloss}},$$

$$L_{xp} = L_{xs}\left(1 + \frac{1}{Q_L^2}\right), \quad (5)$$

$$r_{plossc} = r_{sloss}\left(1 + Q_L^2\right).$$

If L_{xp} is satisfying Eq. 4 then thanks to the parallel resonant tank C_0 and L_{xp} are resonated out and only the parallel connection of the inductor loss resistance r_{ploss} and the transducer emission resistance R_m remain. If high inductor quality is achieved (~100) then the mentioned effects can be disregarded and only the emission resistance R_m is remaining.

If other operation frequency is desired or R_m and C_0 values are not available, then the measured complex impedance can be used instead. Example of air-coupled ultrasonic transducer impedance measurement [11] results is presented in Fig.4.

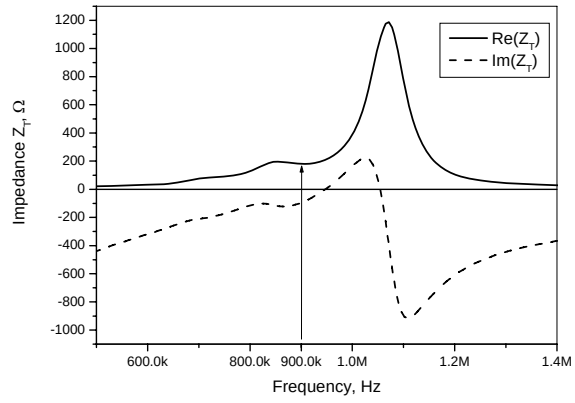

Fig. 4. **Measured electrical impedance of ultrasonic transducer**

The arrow in Fig. 4 indicates the desired operation frequency. Since the impedance presented has a serial connection of real and imaginary parts, these have to be converted to the parallel connection:

$$R_{par} = \mathrm{Re}(Z_T)\left[1 + \left(\frac{\mathrm{Im}(Z_T)}{\mathrm{Re}(Z_T)}\right)^2\right],$$

$$X_{par} = \mathrm{Im}(Z_T)\frac{\left[1 + \left(\frac{\mathrm{Im}(Z_T)}{\mathrm{Re}(Z_T)}\right)^2\right]}{\left(\frac{\mathrm{Im}(Z_T)}{\mathrm{Re}(Z_T)}\right)^2}. \quad (6)$$

Then

$$L_{par} = -\frac{1}{\omega_s X_{par}\big|_{\omega=\omega_s}}. \quad (7)$$

The frequency ω_s used in Eq. 7 can be replaced by other that the series resonance. Again, if the inductor used has a sufficient quality the only remaining part is the real part of the transducer complex impedance parallel equivalent R_{par} obtained from Eq. 6. Otherwise, the inductor quality has to be taken into account using Eq. 5.

The resulting input impedance Z_{in} for the same transducer as in Fig.4 impedance after parallel inductance matching is presented in Fig.5.

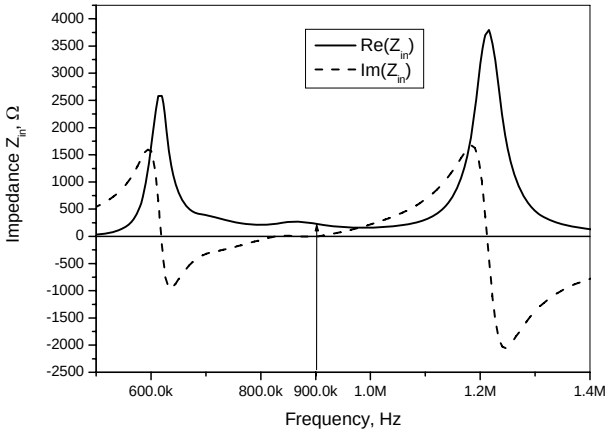

Fig. 5. **Impedance after parallel inductance compensation**

Note that at the desired frequency (indicated by the arrow) the imaginary part was fully compensated.

Serial compensating inductor (Fig.6). Here, the C_0 *serial equivalent* is creating the serial resonant tank with a compensating inductor.

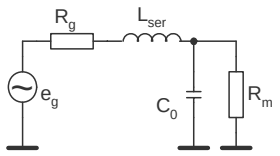

Fig. 6. **Equivalent circuit with series compensating inductance**

Therefore, the transducer impedance at the mechanical resonance has to be converted to a serial form:

$$R_{ser} = \frac{R_m}{1 + (R_m \omega_s C_0)^2},$$

$$X_{ser} = \frac{R_m^2}{\omega_s C_0\left[1 + (R_m \omega_s C_0)^2\right]}. \quad (8)$$

The serial L_{ser} inductance value then is calculated as:

$$L_{ser} = -\frac{1}{\omega_s X_{ser}}. \quad (9)$$

Again, if other frequencies are used or only impedance measurement results are available (refer Fig.3) then the imaginary part of the measured impedance is used:

$$L_{ser} = \frac{1}{\omega_s \mathrm{Im}(Z_T)}. \quad (10)$$

Such compensation results for the same transducer are presented in Fig.7.

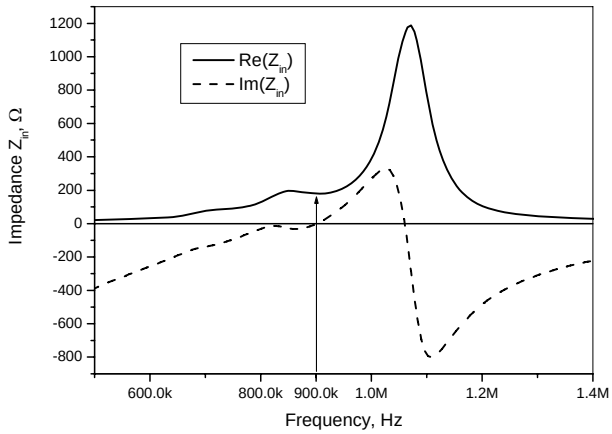

Fig. 7. **Impedance after series inductance compensation**

In this case the inductor quality will influence the remaining real part of the impedance. At the frequency where compensation is used only serial connection of impedance serial form real part and inductor losses resistance r_{sloss} can be regarded as the excitation generator load.

The use of *"L" matching* [12] allows matching both real and imaginary parts. It is implemented by placing two reactive components between the amplifier and the transducer (Fig 8).

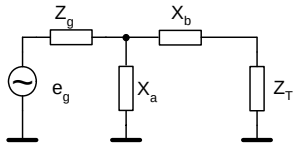

Fig. 8. **Impedance after "L" matching**

The transducer impedance at the desired frequency is converted to a serial form using Eq.8. Then, the corresponding reactances are:

$$X_a = -\frac{R_g^2 + X_g^2}{QR_g + X_g},$$
$$X_b = Q\,\mathrm{Re}(Z_T) - \mathrm{Im}(Z_T), \qquad (11)$$

where

$$Q = \pm\sqrt{\frac{R_g}{\mathrm{Re}(Z_T)}\left[1+\left(\frac{X_g}{R_g}\right)^2\right]} - 1\,. \qquad (12)$$

Taking both Q solutions and swapping source and load positions four configurations are available. Note, that the generator can be treated here as having a complex intrinsic impedance. If the generator output is purely resistive then X_g can be omitted. The results are presented in Fig.9 of resulting input impedance when "L" matching is used for the transducer analyzed above.

The generator output impedance was assumed to be only real 50 Ω resistance. Note, that the imaginary part has been compensated and the real part matched to the generator intrinsic impedance.

Application of *transformer matching* (Fig.10) is a popular technology in RF technique [13].

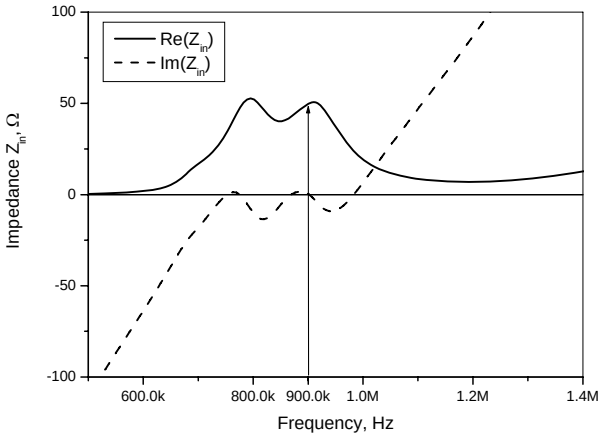

Fig. 9**. Impedance after "L" matching**

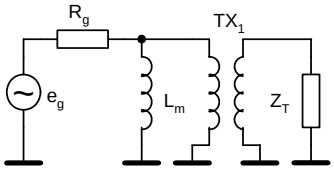

Fig. 10. **Idealized transformer matching circuit**

The idealized transformer presented in Fig.10 is characterized only by turns ratio n and the magnetizing inductance L_m. Such circuit is not complete. For extensive analysis a full transformer model should be used [14, 15]. The magnetizing inductance L_m is defining the lowest applicable frequency. In general it should be chosen so that the reactance at the mechanical resonance is ten times than larger the source impedance:

$$L_m = \frac{10R_g}{\omega_s}. \qquad (13)$$

The impedance is transformed as n^2 therefore the required turns ratio is

$$n = \sqrt{\frac{|Z_T|}{R_g}}. \qquad (14)$$

Eq. 14 is maximizing the power delivered to a complex load. It should be noted that the imaginary part of the load will "tamper" the real part preventing the full available power delivery to the real part of the load. The techniques described above should be used to negate the imaginary part. The graphs in Fig.11 present the matching result or all mentioned techniques. The original impedance

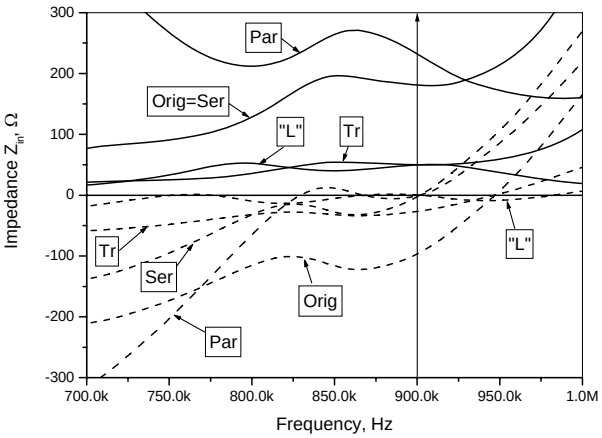

Fig. 11. **Impedance changes after compensations**

curves are labeled as “Orig”, the serial and parallel inductance matching are labeled “Ser” and “Par” correspondingly, “L” label is for “L” matching and “Tr” for transformer matching. The arrow indicates the desired operation frequency.

It should be noted that all techniques except the transformer matching have compensated an imaginary part. Only two techniques (“L” and transformer matching) convert the transducer impedance to desired 50 ohms.

The evaluation criteria

The graphs in Fig.11 are of little use since there is no evident advantage of any matching technique. Therefore we indicate the need for quantitative evaluation criteria. For instance in [9] it was indicated that decision when to use an additional inductance in series or in parallel can be based on the transfer coefficient at the operation frequency.

We define the following evaluation criteria:

- power delivered to a load at the operation frequency;
- -3dB bandwidth [16], effective bandwidth;
- power delivery to load efficiency [17];
- power factor,
- total efficiency.

The complex power delivered to a load can be calculated using the modified input impedance:

$$S_T = \frac{e_g^2 Z_{in}}{\left(R_g + Z_{in}\right)\left(R_g + Z_{in}^*\right)}, \qquad (15)$$

where Z_{in} is the input impedance after matching circuit was applied, Z_{in}^* is the complex conjugate, e_{g} is the generator open-circuit voltage. Assuming that losses in a matching circuit are negligible the real part P_{T} of this complex power S_{T} is equal to the power dissipated in the real part of the transducer acoustic impedance [18]. As it was mentioned before this power can be assigned to acoustic emission of the transducer [19]. The results of investigation are presented in Table 1.

Table 1. **Matching circuit evaluation results**

Circuit	P_T, [mW]	B_{-3dB}, [kHz]	B_{eff}, [kHz]
No matching	2.91	272	365
Series inductance	3.4	287	370
Parallel inductance	2.94	276	364
“L” matching	5	376	366
Transformer	4.68	355	375

The other criterium candidate we define is the -3dB bandwidth of real power P_{T}. The results presented in Table 1 can be obtained using graphs on Fig.12.

The effective bandwidth is adopted from radiolocation as other alternative criteria [20]:

$$B_{eff} = \sqrt{\frac{\int_{f_1}^{f_2} f^2 P_T(f)\,df}{2\pi \int_{f_1}^{f_2} P_T(f)\,df}}. \qquad (16)$$

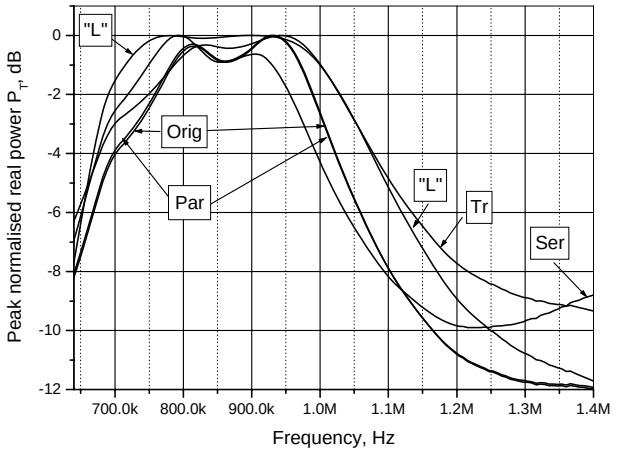

Fig. 12. **Normalized real power**

The results obtained for the effective bandwidth are presented in Table 1. Notable, that series inductance and the matching transformer have produced slightly wider effective bandwidths. The effect can be explained when examining the graphs on Fig.12: both mentioned circuits have a higher real power level at high frequencies.

It is interesting to investigate efficiency of the power delivery to a load is expressed as a real power conveyed to the load ratio to the power available from generator:

$$\eta = \frac{4R_g\,\mathrm{Re}(S_T)}{e_g^2}100\% = \frac{4R_g Z_{in}}{\left(R_g + Z_{in}\right)\left(R_g + Z_{in}^*\right)}100\%\,. \qquad (17)$$

The results of a power delivery to the load efficiency for all mentioned matching techniques are presented in Fig.13.

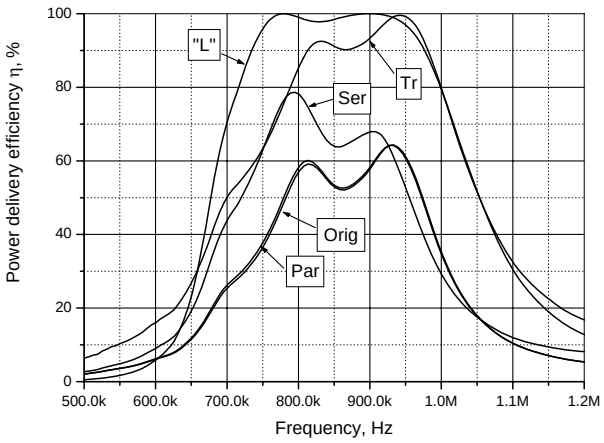

Fig. 13. **Power delivery to load efficiency**

An other widely used criterion is the power factor which is defined as the real power ratio to the apparent power:

$$PF = \frac{\mathrm{Re}(S_T)}{|S_T|} = \frac{\mathrm{Re}(S_T)}{\sqrt{\mathrm{Re}(S_T)^2 + \mathrm{Im}(S_T)^2}}\,. \qquad (18)$$

The results of the power factor evaluation for all mentioned matching techniques are presented in Fig.14.

Analysis of the power factor and the real power delivery efficiency indicate that the same matching technique behave differently according to the analyzed criteria. For instance, the parallel inductance matching has a widest bandwidth according to the power factor, but it has the

same performance as in an unmatched case according to the real power delivery efficiency criterion. Therefore, it is suggested to use the total efficiency criterion:

$$\gamma = PF \cdot \eta \,. \tag{19}$$

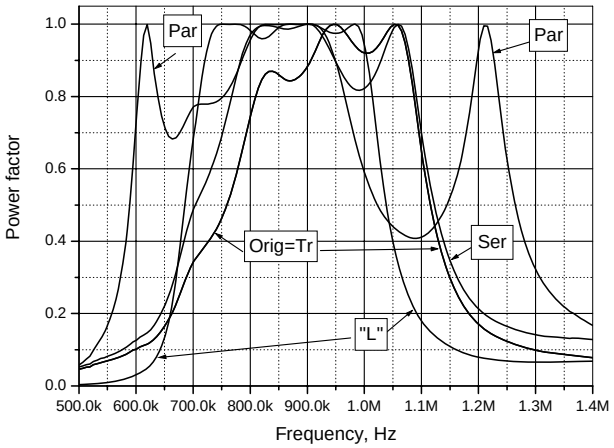

Fig. 14. **Power factor**

Graphs of the total efficiency for the mentioned matching techniques are presented in Fig.15.

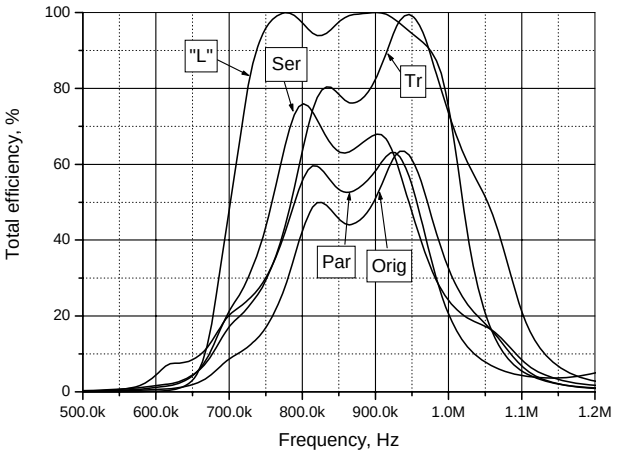

Fig. 15. **Total efficiency**

Now differences between various matching techniques are clearly seen. The total efficiency for an unmatched transducer at the operation frequency (900 kHz) is 50%. When the series inductor matching is used, the total efficiency is increased to 58%. For a parallel matching inductance it is 64%. Application of only one reactive component does not match both real and imaginary impedance parts. Therefore, the total efficiency is lower. Use of "L" matching implies two reactive components. Therefore, the total efficiency is increased to 100% at the operation frequency. For a particular ultrasonic transducer, used for analysis in this paper, "L" matching components have been calculated using the swapped load and the source case:

$$Q_{swp} = \pm\sqrt{\left(\frac{\mathrm{Re}(Z_T)}{R_g}\left[1+\left(\frac{\mathrm{Im}(Z_T)}{\mathrm{Re}(Z_T)}\right)^2\right]-1\right)}. \tag{20}$$

$$X_a = -\frac{|Z_T|^2}{-Q_{swp}\,\mathrm{Re}(Z_T)+\mathrm{Im}(Z_T)},\; X_b = -Q_{swp}R_g \,. \tag{21}$$

Then values for the circuit presented in Fig. 16 are calculated as

$$L_a = \frac{X_a}{\omega_s},\; C_b = \frac{1}{X_b\omega_s}. \tag{22}$$

Such configuration has been chosen deliberately in order to have a high pass filter. If voltage step excitation is used such signal contains significant amount of low frequency components. The high-pass filter prevents those low frequency components to pass to a transducer.

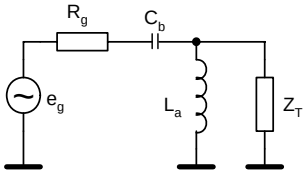

Fig. 16. **"L" matching circuit for particular transducer**

Here "L" matching circuit behaves like a filter where some of filter reactive components are absorbed from a complex parasitic transducer impedance.

If the transformer matching is used to match the real generator output impedance to the magnitude of a complex transducer impedance (Eq. 14) then the total efficiency should not be expected to reach 100%. So, in the analyzed case – the total efficiency is slightly above 80%. This is because the imaginary part is "tampering" the real part. The imaginary part can be compensated using serial or parallel inductance technique. Circuit diagrams for such matching configuration are presented in Fig. 17.

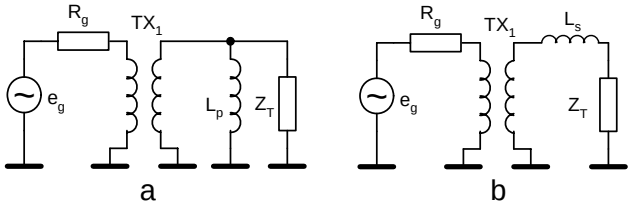

Fig. 17. **Transformer matching combined with parallel (a) or series (b) inductance**

Here the inductor is used for imaginary part compensation and the transformer is used to match the generator output impedance to the real impedance part of the load. Notable, that for the circuit in Fig.17 (a) the inductance Lp can be replaced by a transformer magnetizing the inductance. The graphs in Fig.18 indicate the total efficiency for the same transducer when the circuits presented in Fig.17 are used. The total efficiency is as high as in the case of "L" matching.

Nevertheless, it can be seen that the "L" matching ensures widest matching bandwidth for a particular transducer. This can be explained by accidental production of effectively coupled tanks system which resulted in bandwidth broadening.

Same matching techniques and the total efficiency performance evaluation has been used for the commercial 40kHz air coupled transducer (Fig.19).

Here matching performance is similar for a transformer alone, the transformer combined the with inductor compensation and the "L" matching case.

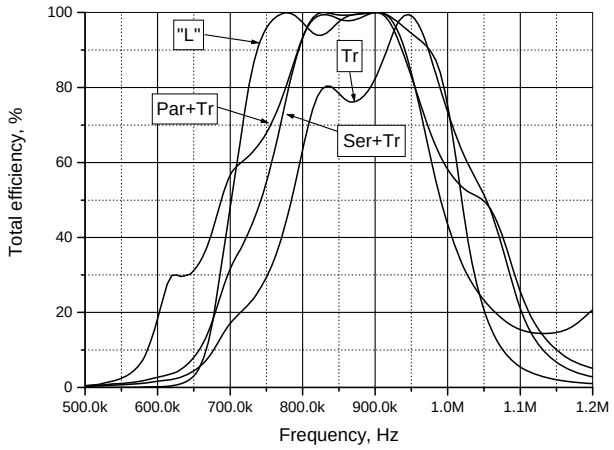

Fig. 18. **Total efficiency for combined matching techniques**

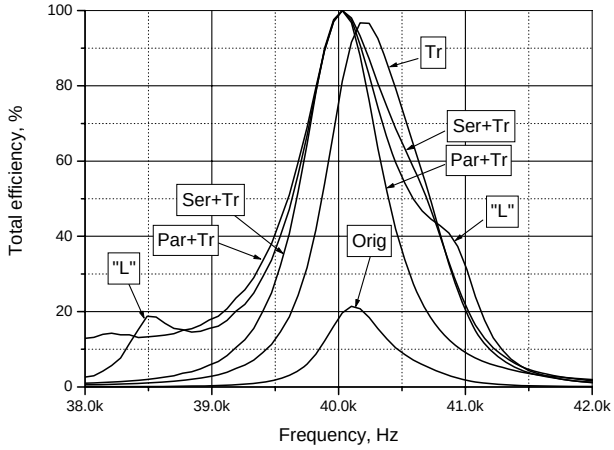

Fig. 19. **Total efficiency for 40kHz commercial transducer**.

Conclusions

It is suggested to use matching performance evaluation based on the measured ultrasonic transducer impedance.

Six matching performance evaluation criteria have been offered. Primary analysis indicates that a total efficiency criterion is sufficient for matching performance evaluation.

References

1. **Ramos A., Emeterio J., Sanz P. T.** Dependence of pulser driving responses on electrical and motional characteristics of NDE ultrasonic probes. Ultrasonics2000. Vol. 38. P.553–558.
2. **Thurston R.** Effect of electrical and mechanical terminating resistances on loss and bandwidth according to the conventional equivalent circuit of a piezoelectric transducer. IRE Trans. on ultrasonic engineering. 1960. P.16-25.
3. **Emeterio J., Ramos A., Sanz P., Ruiz A.** Evaluation of impedance matching schemes for pulse-echo ultrasonic piezoelectric transducers. Ferroelectrics. 2002. Vol.273. P. 297-302.
4. **Capineri L., Masotti L., Rinieri M., and Rocchi S**. Ultrasonic transducer as a black-box: equivalent circuit synthesis and matching network design. IEEE Transactions on ultrasonics, ferroelectrics and frequency control. 1993. Vol. 40. P.694-703.
5. **Sherrity S., Wiedericky H. D., et. al.** Accurate equivalent circuit for the unloaded piezoelectric vibrator in the thickness mode. J. Phys. D: Appl. Phys. 1997. Vol.30. P. 2354–2363.
6. **Prokic M.** Piezoelectric transducers modeling and characterization M.P. Interconsulting. 2004. P.240.
7. **Kauczor C., Frohleke N.** Inverter topologies for ultrasonic piezoelectric transducers with high mechanical Q-factor. Conf. proc. IEEE Power Electronics Specialists. 2004. P.2736-2741.
8. **Mizutani Y., Suzuki T. et. al.** Power maximizing of ultrasonic transducer driven by MOS-FET inverter operating at 1 MHz industrial electronics. Proceedings of the 1996 IEEE IECON Control and Instrumentation. 1996. Vol.22. P.983-986.
9. **Domarkas V., Kazys R.** Piezoelectric transducers for measuring devices. Vilnius: Mintis. 1975. P. 255.
10. **Dumbrava V., Svilainis L.** Measurement of complex permeability of magnetic materials. Measurements. 2006. Vol.37. P.27-32.
11. **Dumbrava V., Svilainis L.** The automated complex impedance measurement system. Electronics and electrical engineering. 2007. Vol.76. P.59-62.
12. **Petersen G.** L-matching the output of a RITEC gated amplifier to an arbitrary load. RITEC Inc., USA. 2006. P.8.
13. **Brounley R. W.** Matching networks for power amplifiers operating into high VSWR loads. HF Electronics. 2004. P.58-62.
14. **Dumbrava V., Svilainis L.** RF transformer parameters measurement. Measurements. 2005. Vol.36. P.22-26.
15. **Svilainis L., Dumbrava V.** The RF transformer application for ultrasound excitation: the initial study. Ultrasound. 2006. Vol.58. P.25-29.
16. **Olcum S., Senlik M. N., Atalar A.** Optimization of the gain-bandwidth product of capacitive micromachined ultrasonic transducers. IEEE Trans. UFFC. 2005. Vol.52. P.2211-2219.
17. **Rhyne T. L.** Characterizing ultrasonic transducers using radiation efficiency and reception noise figure. IEEE Trans. UFFC. 1998. Vol.45. P. 559-566.
18. **Sertbas A. and Yarman B. S.** A computer-aided design technique for lossless matching networks with mixed, lumped and distributed elements. Int. J. Electron. Commun. 2004. Vol.58. P.424-428.
19. **Khmelev V., Savin I. et. al.** Problems of electrical matching of electronic ultrasound frequency generators and eElectroacoustical tTransducers for ultrasound technological installations. Proc. 5th International Siberian workshop and tutorial. 2004. P.211-215.
20. **Skolnik M. I.** Radar handbook. McGraw-Hill Professional. 1990.

L. Svilainis,V. Dumbrava

Ultragarsinio keitiklio elektrinio suderinimo efektyvumo vertinimas

Reziumė

Pateikiama ultragarsinių keitiklių derinimo su žadinimo generatoriumi efektyvumo analizė. Tyrimai atlikti remiantis ultragarsinio keitiklio išmatuota pilnutine varža. Aktyvioji galia, patenkanti į ultragarsinį keitiklį, naudojama kaip vienas iš vertinimo kriterijų. Pasiekiama pralaidos juosta ir jos sandauga su aktyvąja galia pasiūlyta kaip alternatyvūs derinimo efektyvumo įverčiai. Radiolokacijoje naudojama efektinė pralaidos juosta pritaikyta kaip vienas iš kriterijų. Labiausiai paplitusios derinimo grandinės buvo analizuojamos pasiūlytų kriterijų atžvilgiu. Pateikti derinimo grandinių parinkimo algoritmai.

Pateikta spaudai 2007-10-12